Electrochemical conversion of CO_2 to HCOOH at tin cathode: development of a theoretical model and comparison with experimental results

Federica Proietto, Alessandro Galia, and Onofrio Scialdone*

Abstract: The electrochemical reduction of pressurized carbon dioxide at tin cathode is considered a very promising process for the production of formic acid. Here the process was studied in an undivided cell with the aim of developing a simple theoretical model. First, a large series of polarization and electrolyses was performed in order to evaluate the kinetic of the process. According to the literature, experimental results can be described by a simple reaction mechanism, which involves the following key stages: (i) mass transfer of CO_2 to the cathode; (i) its adsorption described by a Langmuir equation; (iii) the reduction of adsorbed CO_2. A simple model was developed based on the cathodic conversion of pressurized CO_2 to HCOOH and on its anodic oxidation. The theoretical model was in a good agreement with experimental results collected in this work and in previous ones and well described the effect of several operative parameters, including current density, pressure and kind of reactor.

1. Introduction

In the last years, many researchers have investigated the electrochemical conversion of CO_2 in water and aprotic solvents to added value products [1-4], including carbon monoxide [5,6], methanol [7,8], formic acid [9-13], methane and ethylene [14,15] and oxalic acid [16,17]. Furthermore, CO_2 can be introduced in the backbone of other molecules, such as benzylic halides and aromatic ketones, generating fine chemicals with high economic value, by cathodic reduction in aprotic solvents [18-22]. One of the more promising chemicals produced by the cathodic reduction of CO_2 in water is the formic acid, despite some disadvantages have to be overcome. Formic acid and formate have a wide application range as antibacterial agent in animal feed and as silage preservative in agriculture, in dyeing, textile and leather industries, in rubber production, as an intermediate in the chemical and pharmaceutical industries and potentially as a fuel and energy-storage medium [23-25]. In addition, the electrochemical route from CO_2 to HCOOH is simple and straightforward and it is expected to have a smaller environmental impact than the current industrial process [26,27]. Sn based electrodes, thanks to low cost, no toxicity and high generation of HCOOH [25-27], are probably the more promising ones for the synthesis of HCOOH [28]. Furthermore, the economics of the process can be drastically improved coupling the cathodic reduction of CO_2 with a suitable anodic process that adds value to the system (such as the anodic purification of wastewater) [24]. Electrochemical conversion of CO_2 into formate/formic acid on Sn electrode was studied under different operative conditions in water [25-35]. One strategy to increase the HCOOH production rate is the utilization of pressurized CO_2, which allows to enhance the carbon dioxide solubility and its reduction rate [36-40]. As an example, some of the authors have recently shown that high concentrations of formic acid (> 0.46 mol L^{-1}) with relatively good current efficiency can be achieved, by reduction of CO_2 at tin cathode and relatively high pressures (15–30 bar), at high current density (> 90 mA cm^{-2}) and with a cheap and simple semi-batch undivided cell with magnetic stirring [39]. Furthermore, the process was successfully scaled-up in a filter-press cell with a continuous recirculation of the pressurized solution [40].

In spite of the good results achieved, many data were not clearly understood; hence, in order to better understand and rationalize the process, a theoretical model was here proposed for the cathodic reduction of pressurized CO_2 at tin cathode.

The electrochemical reduction of CO_2 must be characterized by high productivity, high selectivity and current efficiency and high final concentrations of HCOOH in order to reduce the concentration costs. Quite often, the high number of operative parameters, which may be changed, makes an empirical investigation exceedingly onerous in order to individuate the conditions which allow to optimize the process. Hence, theoretical predictions/mathematical models offer promising strategies to select the best experimental conditions to be tested. The experimental validation of mathematical models can, furthermore, confirm the assumptions on which the model is based and allow to describe the process. For these reason, various models have been developed in recent years to describe the electrochemical conversion of CO_2 [13,41,42], based on different reaction mechanisms proposed in literature [4,36,43-46]. However, the models were not focused on the utilization of pressurized CO_2 and in most of cases were devoted to divided cells, in spite of the fact that undivided ones are less expensive. Hence, here a simple first-approximation model was developed based on one hand on the cathodic conversion of pressurized CO_2 to HCOOH and on the other on its anodic oxidation. In order to develop the model, many preliminary experiments were performed to find the r.d.s. of

Eng. F. Proietto, Prof. A. Galia, Prof. O. Scialdone
Dipartimento dell'Innovazione Industriale e Digitale – DIID
Ingegneria Chimica, Gestionale, Informatica, Meccanica.
Università degli Studi di Palermo.
Viale delle Scienze, Ed. 6, 90128 Palermo, Italy
E-mail: onofrio.scialdone@unipa.it

the process. It is worth to mention that the utilization of pressurized CO_2 allowed to collect useful data in order to describe the kinetic of the process. After, the model was compared with experimental data collected both in this work and in previous ones and a good agreement between experimental results and theoretical predictions was observed.

2. Results and Discussion

2.1 Polarization and electrolysis experiments and discussion of reaction mechanism

First, a preliminary series of polarization and electrolyses was performed both a 1 bar and under pressure to achieve information on the mechanism in order to develop a simplified theoretical model.

2.1.1 Effect of pH and current density

Fig. 1 reports polarization experiments recorded at different pH values. At pH 4 (fig. 1a), the hydrogen evolution starts at a potential of about -1.55 V (vs. SCE) and the dependence of the current density vs. the potential becomes more relevant at potentials slightly more negative than -2 V. The hydrogen evolution is expected to take place by the following reactions:

(i) cathodic reduction of protons to adsorbed H

$$H^+ + e^- = H_{(ads)} \quad (1)$$

(ii) evolution of hydrogen by

$$H_{(ads)} + H^+ + e^- = H_2 \quad (2a)$$

or

$$H_{(ads)} + H_{(ads)} = H_2 \quad (2b)$$

According to Azizi et al. [49] at tin in acidic conditions and low negative potentials, the Heyrovsky step (eq. 2a) prevails on Tafel one (eq. 2b), it is the r.d.s. (e.g. $r_1 > r_{2a} > r_{2b}$) and the superficial coverage by adsorbed hydrogen is negligible. Conversely, at high negative potentials, the surface coverage of the electrode by adsorbed hydrogen reaches a higher value and the mechanism of the HER is a consecutive combination of Volmer and Heyrovsky steps with equal rates, the rate of Tafel reaction being negligible (e.g. $r_1 \sim r_{2a} > r_{2b}$).

When CO_2 is added to the system (at 1 bar), an increase of the current is observed for potentials close to -1.5 V (fig.1a). The difference between the overall current and the current recorded in the absence of CO_2, called j_{CO_2}, increases up to about -1.8 V (fig. 1d); it assumes an almost constant value for a potential between -1.8 and about -2.05 V and decreases for more negative potentials. When CO_2 is removed from the system, the current density comes back again to the values recorded during the first polarization recorded under N_2 atmosphere. A similar behaviour was observed at pH 3 (fig. 1b) and 2 (fig.1c), even if at pH 2 the hydrogen evolution starts at a potential of about -1.1 V (vs. SCE). As shown in fig. 1d, at all pH the maximum value of j_{CO_2} is close to the limiting current density j_{lim} estimated for a process under the kinetic control of the mass transfer in the absence of mixing. Fig. 1e reports the cyclic voltammogram achieved at pH 4 and 30 mV s^{-1}; the anodic peaks between −0.75 and −1 V and the cathodic peak at about −1.1 V, which can be attributed to the formation and the reduction of tin oxides respectively, are partially suppressed under CO_2 atmosphere. Furthermore, the addition of CO_2 gives rise to a shoulder at potentials close to -2.0 V and also in this case, for very negative potentials, j_{CO_2} decreases with the potential (fig. 1e, inset).

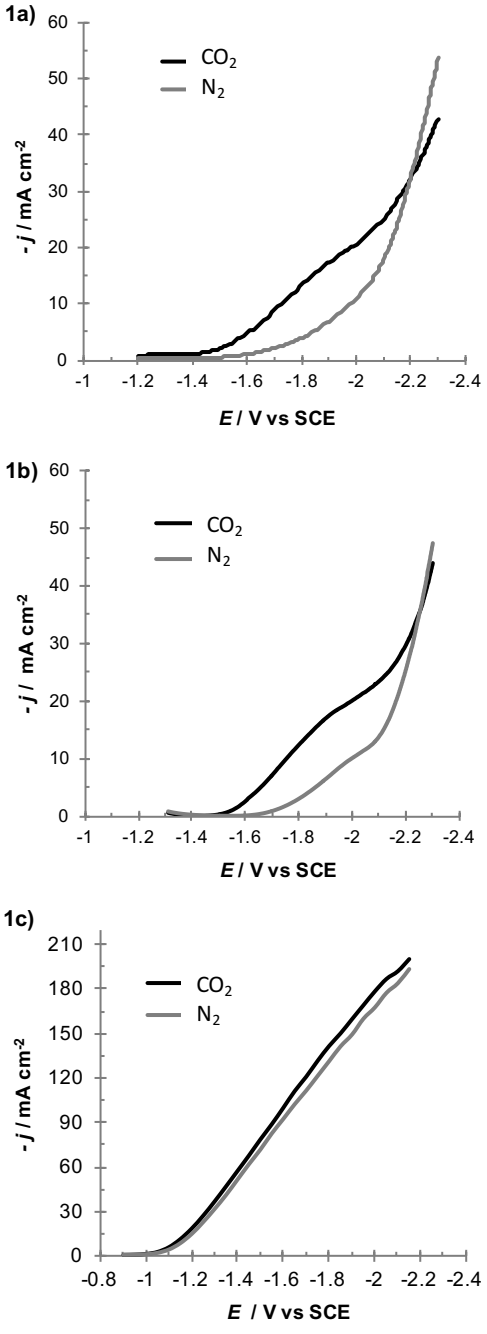

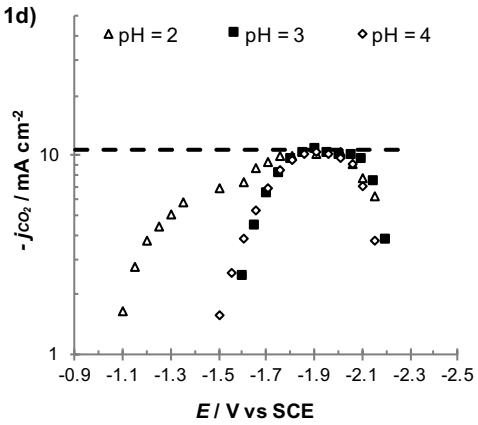

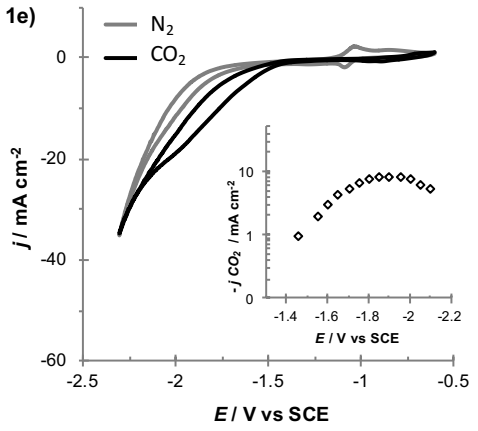

Figure 1. LSVs at 5 mV s^{-1} under 1 bar N_2 (grey line) and CO_2 (black line)-saturated water solution of 0.1 M Na_2SO_4 at (1a) pH = 4, (1b) pH = 3 and (1c) pH = 2. (1d) Comparison of the CO_2 partial current density at different pH values. (1e) CV at 30 mV s^{-1} under N_2 (grey line) and CO_2 (black line)-saturated solution of 0.1 M Na_2SO_4 at pH = 4. Volume of the solution (V): 0.05 L. $A_{cathode}$ = 0.1 cm^2.

In order to achieve more data on the effect of current density *j* on the cathodic reduction of CO_2, a series of amperostatic electrolyses was performed at pH 4 with 1 bar of CO_2 changing *j* from 7.8 to 80 mA cm^{-2} (fig. 2a and 2b). In all cases, the main product of carbon dioxide reduction was formic acid and only very low amounts of CO were detected. It is worth to mention that, according to polarization, CV experiments and the literature [39], the current density dramatically affects both the rate of production of formic acid and the current efficiency (*CE*). Indeed, the curve HCOOH production rate vs. *j* (fig. 2a) gave a maximum for 20 mA cm^{-2} (very close to the j_{lim} = 22 mA cm^{-2} for adopted operating conditions) while *CE* decreases with *j* in all the range of adopted current density (fig. 2b), since higher current densities give rise to a higher contribution of the parasitic process of hydrogen evolution.

In order to explain the experimental results achieved, the reaction mechanism proposed by several authors for CO_2 reduction at tin cathode [34,38,41,44] can be considered:

(i) mass transfer of dissolved CO_2 to the cathode surface (whose rate is given by k_m ($[CO_2]^b$-$[CO_2]^0$), where $[CO_2]^b$ and $[CO_2]^0$ are the concentrations of CO_2 in the bulk and at the electrode surface, respectively, and k_m is the mass transfer coefficient for CO_2)

(ii) adsorption of CO_2

$$CO_{2_{(aq)}} = CO_{2_{(ads)}} \quad (3)$$

(iii) cathodic reduction of adsorbed CO_2 to adsorbed $CO_2^{\bullet-}$

$$CO_{2_{(ads)}} + e^- = CO_{2_{(ads)}}^{-\cdot} \quad (4)$$

(iv) cathodic reduction of adsorbed $CO_2^{\bullet-}$ to HCOOH

$$CO_{2_{(ads)}}^{-\cdot} + H^+ = HCO_{2_{(ads)}} \quad (5)$$

$$HCO_{2_{(ads)}} + H^+ + e^- = HCOOH \quad (6)$$

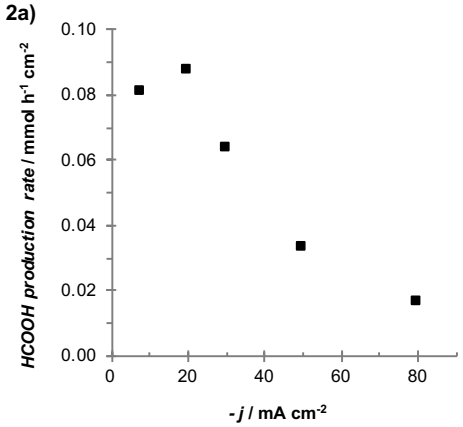

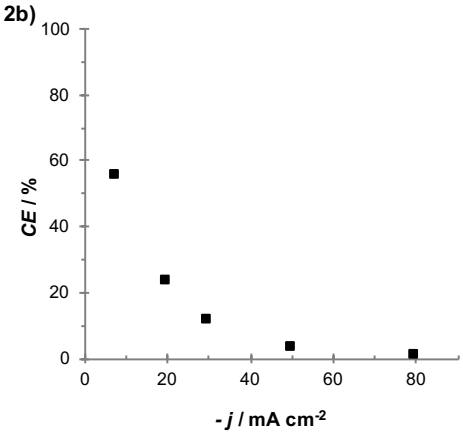

Figure 2. Effect of the current density on the formic acid production rate (2a) and current efficiency (2b). Electrolyses performed in a pressurized filter-press cell equipped with Sn cathode (9 cm^2) under amperostatic condition, fixed CO_2 pressure (1 bar) and a constant flow-rate value (200mL min^{-1}). Volume of the solution (V): 0.9 L. Time: 2h.

According to this reaction mechanism and to experimental data reported in fig. 1 and 2, in the polarization curves recorded at pH 3 and 4, four relevant regions can be considered:

1) Region 1. For not sufficiently negative potentials (E > -1.5 V vs SCE), CO_2 reduction does not take place in a significant way (j < 1 mA cm^{-2}) for kinetic reasons. According to the literature [38] for these very low current densities, the r.d.s. would be the second electron transfer (eq. (6)).
2) Region 2. For potential values between -1.5 and -1.75 V, the more negative is the potential the higher is j_{CO_2}. The slope of the Tafel curve has a value of ca. -352 mV. According to Vassiliev et al. [38], under these conditions, the process is limited by the first electron transfer (eq. (4)).
3) Region 3. For potentials between -1.75 V and -2.1 V, j_{CO2} reaches a maximum value which is close to j_{lim}, since the process is under the kinetic control of the mass transfer of CO_2 to the cathode surface.
4) Region 4. For potentials more negative than -2.2 V, j_{CO2} decreases with the potential. A similar behaviour was observed in literature [38] but not commented in detail. Under these conditions, the cathodic reduction of water (eq.ns (1-2)) is expected to be very fast, thus limiting or suppressing the formation of HCOOH for various reasons: (i) the H coverage is expected to increase, thus limiting the rate of CO_2 adsorption (see eq. 3); (ii) the concentration of protons at the tin surface is expected to decrease, thus reducing the rate of both eq.ns (5) and (6); (iii) the high hydrogen evolution can cause a partial covering of the electrode surface, thus decreasing the rate of the mass transfer of CO_2 to the cathode. In particular, by assuming a competition between the adsorption of CO_2 and H, this region is expected to be shifted to more negative potentials by both higher mixing rates or higher CO_2 pressures.

2.1.2 Effect of mixing rate and CO_2 pressure

In order to better characterize the process and the reaction scheme proposed in the previous paragraph, a series of polarizations and electrolyses was performed at pH 4 at different mixing rates and CO_2 pressures. First, some polarization and electrolyses were performed at 1 bar and different rpm. For polarizations, a curve with a maximum was obtained for j_{CO_2} for all rpm (fig. 3a); j_{CO_2} did not depend on rpm for E > -1.75 V (j_{CO_2} < 6 mA cm^{-2}), when the process is not limited by the mass transfer of CO_2 to the cathode (regions 1 and 2), while it increased with the mixing rate for more negative values of E, when the process is kinetically influenced by the mass transfer, according to the picture depicted in the previous paragraph. In particular, the maximum values of j_{CO_2} achieved at different rpm are closer (even if slightly lower) to the corresponding estimated values of j_{lim}. Electrolyses were performed at 11.6 mA cm^{-2}, a value slightly higher than $j_{lim.}$ estimated in the absence of mixing rate. As shown in fig. 3b, the enhancement of rpm increases the formic acid production and the current efficiency. In particular, the rate of production of formic acid after 1h increases from about 0.08 to 0.11 millimoles h^{-1} cm^{-2} and *CE* from about 39 to 48 % enhancing the rpm from 0 to 600, according to results of polarization curves.

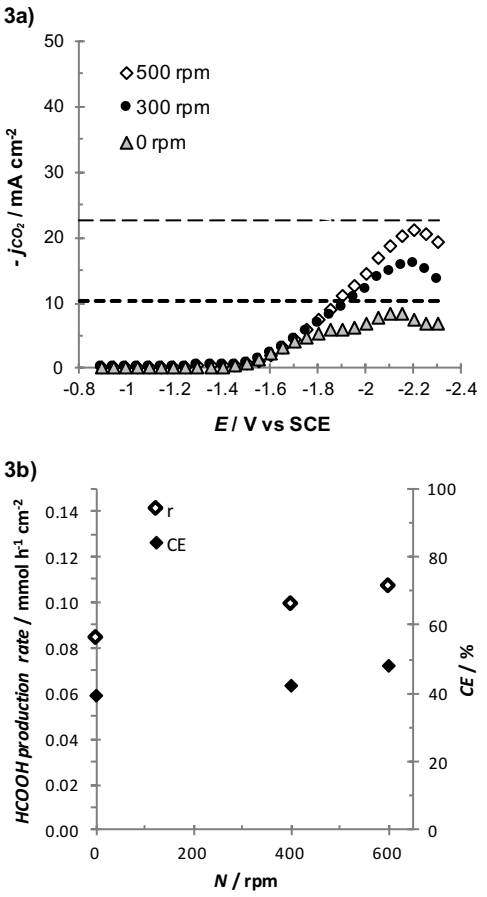

Figure 3. Effect of the mixing rate on the CO_2 partial current density (3a). The dotted lines are referred to the limit current density evaluated at 0 (---) and 500 (— — —) rpm. The relative polarizations were performed in a conventional lab cell. Volume of the solution (V): 0.05 L. $A_{cathode}$= 0.1 cm^2. (3b) Effect of the mixing rate on the formic acid production rate and on CE. Electrolysis performed in a conventional-lab glass cell equipped with Sn cathode (4.5 cm^2) under amperostatic condition, (11.6 mA cm^{-2}) and atmospheric CO_2 pressure. Volume of the solution (V): 0.075 L. Time: 1h.

In order to evaluate the effect of the CO_2 concentration in water on the CO_2 reduction, current densities were recorded as a function of cell potential in the presence of N_2 and with different pressures of CO_2 in the range 1 – 30 bar. As shown in fig. 4a, for each value of P_{CO_2}, a similar curve j_{CO_2} vs. ΔV characterized by the presence of a maximum is observed, thus showing the existence of four regions in polarization curves also for pressurized systems. In particular, for not too negative potentials, j_{CO_2} increases with the pressure even if the enhancement becomes very small for the highest P_{CO_2}. Vassiliev at al. [38] have shown that the rate of CO_2 electroreduction at various electrodes including tin increases proportionally to a fractional power of P_{CO_2}. According to these authors, the fractional order of the reaction indicates that the rate-determining steps of the reaction involve adsorbed molecules and there is a strongly repulsion between them.

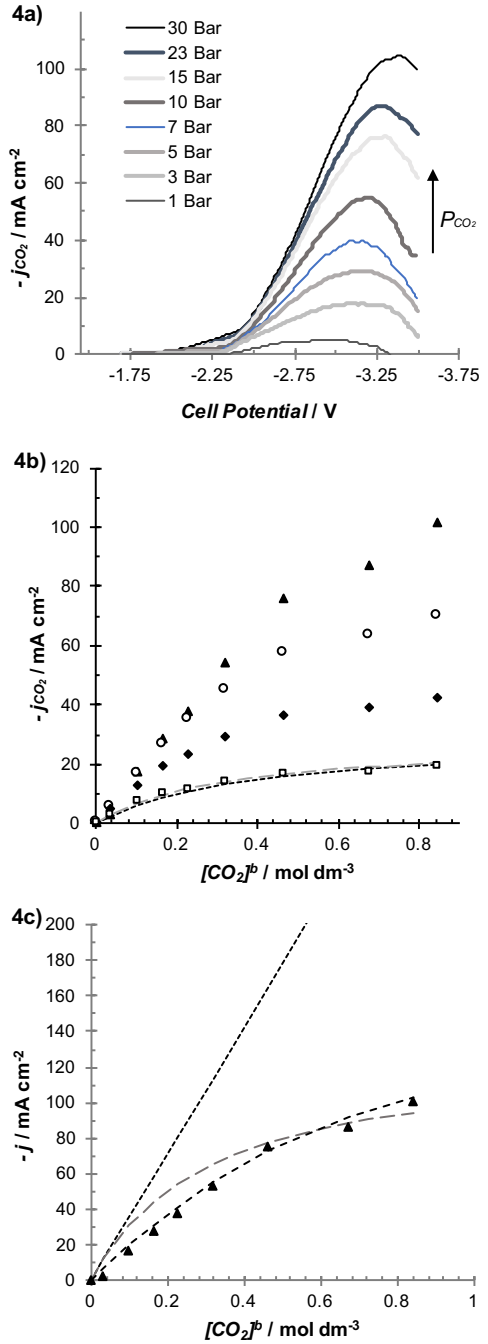

Figure 4. (4a) CO_2 partial current density recorded by polarizations achieved at different CO_2 pressure. (4b) CO_2 partial current density shown in fig. 4a plotted versus the bulk CO_2 concentration at different cell potentials: -2.55 V (□), -2.75 V (♦), -2.95 V (○) and -3.25 V (▲). Data achieved at -2.55 V are compared with theoretical predictions based on the Langmuir-Hinshelwood expression (— —) or on a mixed kinetic control of the mass transfer of CO_2 to the cathode surface and of the reduction of adsorbed CO_2 (where adsorption is described by the Langmuir expression) (- - -). (4c) Data of fig. 4b achieved at -3.25 V (▲) are compared with the limiting current density (---), the theoretical predictions based on Langmuir-Hinshelwood expression (— —) and on a mixed kinetic control of the mass transfer of CO_2 to the cathode surface and of the reduction of adsorbed CO_2 (described by the Langmuir expression) (- - -). Pseudo-LSVs were performed in a stainless steel cell at 5mV s^{-1} in water solution of 0.1M Na_2SO_4 at pH = 4. Volume of the solution (V): 0.05 L. $A_{cathode}$ = 0.1 cm^2.

Also in our case, experimental data indicate that the r.d.s. involve adsorbed molecules even if, as shown in fig. 3b, they can be better fitted by a Langmuir-Hinshelwood type expression (r = *k(E)* b $[CO_2]/(1+b\ [CO_2])$; indeed, j_{CO_2} increases proportionally to C_{CO_2} for lower values of P_{CO_2} and tend to a plateau value for high values of P_{CO_2}. As shown in fig. 4b, a quite good fitting with a Langmuir-Hinshelwood expression is obtained for not very negative values of the potential (ΔE = -2.55 V; region 2), thus reinforcing the hypothesis that the r.d.s. in the region 2 is the cathodic reduction of adsorbed CO_2 to adsorbed $CO_2^{\bullet-}$ (eq. (4)) and indicating that the adsorption of carbon dioxide can be assumed at the equilibria and described by the Langmuir model. In particular, according to the fitting reported in fig. 3b for region 2, the coverage of the surface by carbon dioxide (θ) can be estimated to change from about 0.08 to about 0.71 increasing P_{CO_2} from 1 to 30 bar. In region 3, the maximum j_{CO_2} was significantly lower than j_{lim} (fig. 4c), thus showing that the r.d.s. for a pressurized system is not the mass transfer even at very negative potentials. A better fitting of the data is obtained (as shown in fig. 4c) using the Langmuir-Hinshelwood expression; however, also in this case the fitting can not be considered excellent. Conversely, the data in region 3 are well fitted considering a process under the mixed kinetic control of the mass transfer of CO_2 to the cathode surface and of the reduction of adsorbed CO_2 (the last, described by the Langmuir-Hinshelwood expression) (fig. 4c). In particular, in this case, the coverage of the surface by carbon dioxide (θ) can be estimated to change from about 0.04 to about 0.64 and the ratio $[CO_2]^b/[CO_2]^\circ$ from 2.4 to 1.5 changing P_{CO_2} from 1 to 30 bar. Hence, the process is more limited by mass transfer and reduction stages, for lower and higher values of P_{CO_2}, respectively.

A series of electrolyses was performed at a relatively high pressure (23 bar) at 30 (region 2) and 160 mA cm^{-2} (region 3-4) at different rpm in order to evaluate the effect of flow-dynamic for relatively high pressures. As shown in fig. 5a and 5b, according to theoretical considerations developed above, the mixing rate had not a significant effect of HCOOH production at the lower current density, while it had an appreciable effect at very high values of *j*. Hence, it can be concluded that for pressurized systems, the process can be described by the reaction mechanism reported in equations (3) – (6) and that in region 3 the process is under the mixed kinetic control of mass transfer of CO_2 and reduction of adsorbed CO_2.

Some authors have proposed that on some electrodes [9,43] the reduction of carbon dioxide can be due a different mechanism based on the reaction between adsorbed H and adsorbed carbon dioxide:

$$H_{(ads)} + CO_{2_{(ads)}} = HCO_{2_{(ads)}} \quad (7a)$$

$$HCO_{2_{(ads)}} + H^+ + e^- = HCOOH \quad (7b)$$

In particular, according to Paik and co-authors [43], this mechanism is likely to be involved at Hg for weakly acidic pH. However, in our case experimental data seem to be more easily described by the reaction mechanism shown in equations 3-6. Hence, this mechanism will not be considered in the following.

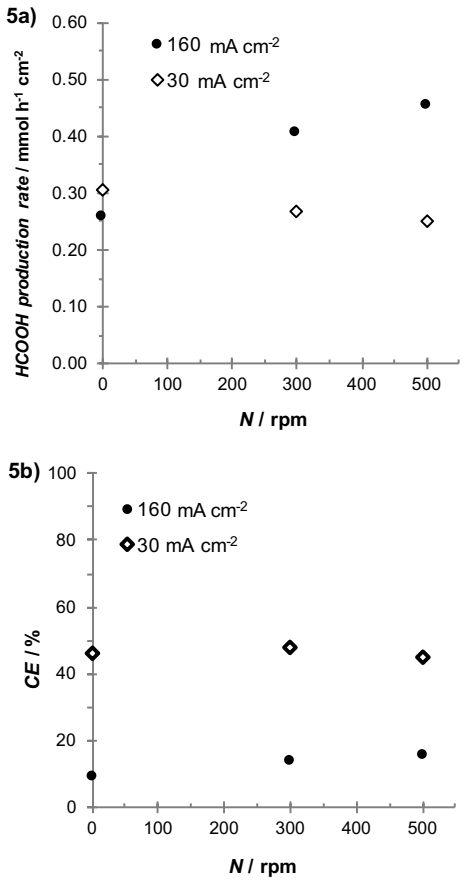

Figure 5. Combined effect of the mixing rate and current density on the HCOOH production rate (5a) and current efficiency (5b). Electrolyses were performed in a stainless steel cell at 5 mV s^{-1} in water solution of 0.1M Na_2SO_4 at pH = 4. Volume of the solution (V): 0.05 L. $A_{cathode}$ = 0.1 cm^2. Time: 1h

2.2 Mathematical model and comparison with experimental results

2.2.1 Theoretical model

In the following, we want to develop a simple theoretical model in order to highlight the expected effect of some operating parameters on the figures of merit of the process. Since we do not want a complete characterization of the process and we want to limit the number of fitting parameters, we will consider a simple first-approximation theoretical model based on various simplified assumptions, cited below, for both the cathodic reduction of carbon dioxide and the anodic oxidation of formic acid. In particular, the rate of HCOOH generation will be estimated as the difference between r_{CO_2} (the rate of cathodic CO_2 conversion to HCOOH) and r_{HCOOH} (the rate of HCOOH oxidation at the anode).

2.3.2 Cathodic reduction of carbon dioxide

According to above considerations, the reduction of CO_2 at tin cathode strongly depends on the adopted potential and current density. We will focus in the following on the current density since for applicative conditions amperostatic electrolyses are preferred.

As shown in the previous paragraph, for too low (region 1) and too high current densities (region 4), the production of formic acid is expected to be small; hence, we will focus our attention on experiments performed in regions 2 and 3, where the highest rates for CO_2 production can be achieved, thus leading to the highest productivity. Furthermore, the following assumptions will be considered.

- The cathodic reduction of carbon dioxide leads to formic acid by the reaction mechanism reported in paragraph 3.1 (equations (3) - (6)). Furthermore, it is assumed that the only competitive process is the cathodic reduction of water. This hypothesis is reasonable since at adopted operating condition only a very minor amount of CO_2 is converted to CO (< 5%) [39,40] and no other products were detected.
- The rate of CO_2 reduction r_{CO_2} takes place under the mixed kinetic control of mass transfer of CO_2 to the cathode and reduction of adsorbed CO_2 (see eq. (4)):

$$r_{CO_2} = k_m ([CO_2]^b - [CO_2]^\circ) = k_4(E)\theta \quad (8)$$

  where the superficial coverage of CO_2 θ is described by Langmuir expression and b is assumed to be constant with the potential:

$$\theta = b\,[CO_2]/(1+b\,[CO_2]) \quad (9)$$

- For the sake of simplicity, the ratio between $k'(E)$ (i.e., the product of the heterogeneous rate constant for the reduction of the water and water concentration) and $k_4(E)$ is considered to assume a constant value.

On the bases of these assumptions, the total current density is expected to be simply given by the sum of the current densities due to the cathodic reduction of CO_2 to formic acid (j_{CO_2}) and of water (j_{wat}), respectively:

$$j = j_{CO_2} + j_{wat} = 2Fk_4(E)\theta + 2Fk'(E) = \\ = 2Fk_4(E)\, b[CO_2]^\circ/(1+b\,[CO_2]^\circ) + 2Fk'(E) \quad (10)$$

where F is the Faraday constant (96487 C mol^{-1}). Hence, the instantaneous current efficiency (*ICE*) can be estimated by the following equation:

$$ICE = \frac{\frac{k_4(E)b[CO_2]^\circ}{(1+b[CO_2]^\circ)}}{\frac{k_4(E)b[CO_2]^\circ}{(1+b[CO_2]^\circ)}+k'(E)} = \frac{\frac{b\,[CO_2]^\circ}{(1+b\,[CO_2]^\circ)}}{\frac{b\,[CO_2]^\circ}{(1+b\,[CO_2]^\circ)}+\frac{k'(E)}{k_4(E)}} \quad (11)$$

which could be approximated to eq. (11b) and (11c) for low and high values of P_{CO_2}, respectively.

$$ICE = \frac{b[CO2]^\circ}{b[CO2]^\circ + k'(E)/k_4(E)} \quad (11b)$$

$$ICE = \frac{1}{1+k'(E)/k_4(E)} \quad (11c)$$

and $[CO_2]^\circ$ can be easily estimated by equating the rate of mass transfer of carbon dioxide and the rate of cathodic reduction of adsorbed CO_2 (eq. 8). Hence, the experimental results will be fitted by theoretical prediction based on eq. (8) and (11) using

$k'(E)/k_4(E)$ and b as fitting parameters, while k_m was estimated by diffusion limiting current technique.

2.2.2 Anodic oxidation of formic acid

Since experiments are performed in an undivided cell, the anodic oxidation of formic acid has to be considered. According to the literature [50,51], the following assumptions will be made for the sake of simplicity to describe the anodic oxidation of HCOOH:

- The oxidation of the organic is assumed to take place only by anodic reactions (e.g., no homogeneous oxidation processes are considered to take place).
- The only competitive process to the oxidation of HCOOH is assumed to be the oxidation of water to oxygen.
- The chemi-adsorption of HCOOH and its oxidation products is negligible or it does not affect significantly the water and HCOOH oxidation rates.
- Furthermore, for the sake of simplicity, the ratio between $k_{an}'(E)$ (i.e., the product of the heterogeneous rate constant for the oxidation of the water and water concentration) and $k_{HCOOH}(E)$ (the heterogeneous rate constant for the oxidation of HCOOH) is considered to assume a constant value.

According to the above mentioned assumptions, the anodic oxidation of formic acid r_{HCOOH} is assumed to take place under the mixed kinetic control of mass transfer of HCOOH to the anode and the anodic oxidation of HCOOH:

$$r_{HCOOH} = k_{m,HCOOH}\,([HCOOH]^b - [HCOOH]^0) = k_{HCOOH}(E)\,[HCOOH]^0 \quad (12)$$

where $k_{m,HCOOH}$ is the mass transfer coefficient for HCOOH and $[HCOOH]^b$ e $[HCOOH]^0$ are the concentrations of HCOOH in the bulk and at the anode surface, respectively.

On the bases of these assumptions, the total current density is expected to be simply given by the sum of the current densities due to the anodic oxidation of formic acid to CO_2 (j_{HCOOH}) and of water ($j_{wat,an}$), respectively:

$$j = j_{HCOOH} + j_{wat,an} = 2F k_{HCOOH}(E)\,[HCOOH]^0 + 2F\,k_{an}'(E) \quad (13)$$

Hence, the instantaneous current efficiency (*ICE*) can be estimated by the following equation:

$$ICE = \frac{k_{HCOOH}(E)[HCOOH]^\circ}{k_{HCOOH}(E)[HCOOH]^\circ + k_{an}'(E)} = \frac{1}{1+\frac{k_{an}'(E)}{k_{HCOOH}(E)[HCOOH]^\circ}} \quad (14)$$

and $[HCOOH]^\circ$ can be easily estimated by equating the rate of mass transfer of HCOOH and the anodic oxidation of HCOOH (eq. 12). Hence, since $k_{m,HCOOH}$ can be estimated by diffusion limiting current technique, the only unknown parameter is $k_{an}'(E)/k_{HCOOH}(E)$, which was estimated as fitting parameter comparing the experimental results and theoretical predictions.

2.3 Comparison with experimental data

2.3.1 Effect of pressure

Some experiments were performed for 4 hours at various pressures (1, 5, 10, 15, 23 and 30 bar) in order to evaluate the effect of the pressure on the generation of HCOOH. A current density j of 20 mA cm^{-2} was selected. At this current density, j_{lim} is higher than j for all the adopted pressure with the exception of 1 bar. Furthermore, for a pressure higher than 3 bar, the process occurs in region 2. As shown in fig. 6, the increase of the pressure from 1 to 5 bar resulted in a strong enhancement of the production of HCOOH (from 2.3 to 5.8 mM after 4 h). A further increase of the concentration of HCOOH was observed upon increasing the pressure up to 23 bar even if the effect of the pressure became less relevant for high P_{CO_2}; furthermore, similar productions of HCOOH were observed for 23 and 30 bar. The experimental results were compared with the theoretical model presented in paragraph 2.2.1. The model fits quite well the experimental trends (fitting parameters $k'(E)/k_4(E)$ = 0.18, $k_{an}'(E)/k_{HCOOH}(E)$ = 0.3 M, b = 1). In particular, the effect of the pressure according to the theoretical model becomes less relevant at the highest adopted values of P_{CO_2} since a higher superficial coverage θ occurs.

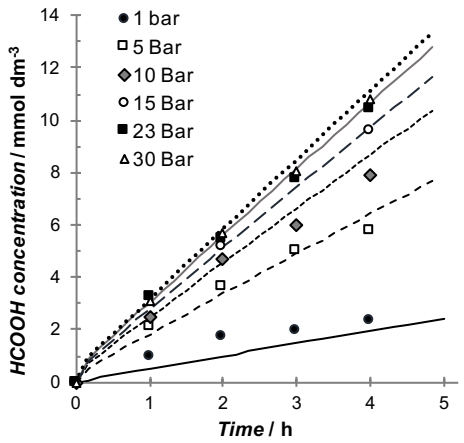

Figure 6. Plot of the formic acid concentration vs time at 20 mA cm^{-2}. Comparison of the experimental [HCOOH] with the theoretical [HCOOH] at several value of pressure: 1 (—); 5(- -); 10 (---); 15 (— — —); 23 (—); 30 (•••) bar. Theoretical [HCOOH] was evaluated under the assumptions described in the section 2.2.1 with the following fitting parameters: $k'(E)/k_4(E)$ = 0.18; $k_{an}'(E)/k_{HCOOH}(E)$ = 0.3 M; b = 1.

2.3.2 Effect of the current density

The effect of current density was first evaluated at 10 (7.8, 20 and 30 mA cm^{-2}) and 23 bar (7.8, 20, 30 and 50 mA cm^{-2}) for 4 hours. Not very high current densities were selected in order to avoid region 4. At both pressures, the higher was j the higher was the production of formic acid (fig. 7). Also in this case, the experimental results were compared with the model, here used entirely in predictive mode since the values of parameters $k'(E)/k_4(E)$, $k_{an}'(E)/k_{HCOOH}(E)$ and b estimated in paragraph 2.2.1 well used. As shown in fig. 7, the model well captured the effect of j at both adopted pressures.

According to the assumptions developed in the model, a similar coverage θ was obtained for the same value of the pressure changing the current density; furthermore, under adopted conditions, the process was slightly limited by mass transfer;

hence quite similar values of *CE* were achieved at all adopted current densities (55 and 68 % at 10 and 23 bar, respectively) that were well predicted by the model.

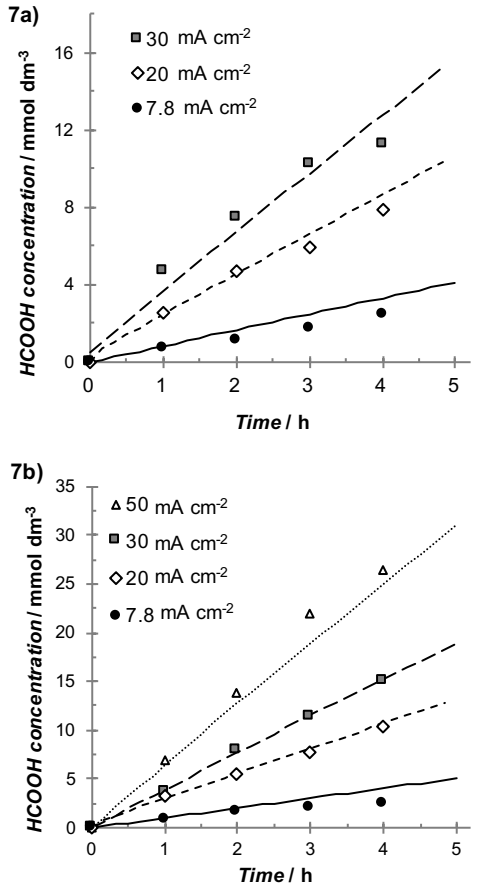

Figure 7. Plot of formic acid concentration vs. time at 10 (7a) and 23 (7b) bar. Comparison of the experimental *[HCOOH]* with the theoretical *[HCOOH]* at several value of current density: 7.8 (—); 20 (– – –); 30 (— —); 50 (•••) mA cm^{-2}. Theoretical [HCOOH] was evaluated under the assumptions described in the section 2.2.1 with the following fitting parameters: $k'(E)/k_4(E)$ = 0.18; $k_{an}'(E)/k_{HCOOH}(E)$ = 0.3 M; b = 1.

As shown in fig. 6 and 7, the plot HCOOH concentration vs. time is almost linear. This is due to the fact that under adopted operating conditions the anodic oxidation of formic acid is quite limited due to the rather low values of [HCOOH]. As an example, at 23 bar and 30 mA cm^{-2}, the ICE for the anodic oxidation of HCOOH after 4 h was estimated to be about 4% in face of an ICE for the HCOOH generation at the cathode close to 70%.

The results of a larger set of experiments obtained changing both pressure (from 1 to 23 bar) and *j* (from 7.78 to 50 mA cm^{-2}) selected in literature [40] in order to work in regions 2 and 3 were reported in fig. 8. In order to put in the same graph all the data, the final concentration of each experiment after 4 h was reported.

It can be clearly observed that for a constant current density the final concentration of HCOOH increases with P_{CO_2} up to a plateau value, which increases with *j*. The data can be rationalized considering that (i) the kinetic is strongly influenced by the rate of the reduction of adsorbed CO_2 which increases with the potential (and the current density) and with the superficial coverage of CO_2 θ; (ii) the dependence of θ by $[CO_2]$ can be described by a Langmuir-type equation and θ is expected to increase with $[CO_2]$ and P_{CO2} up to a plateau value.

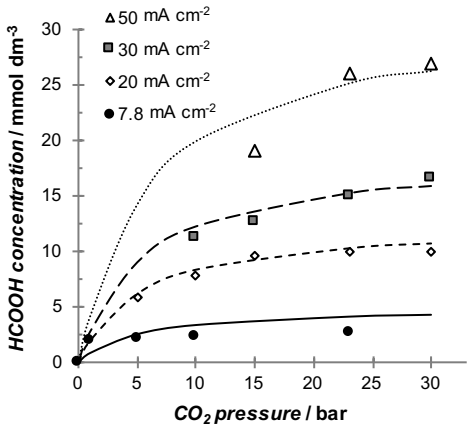

Figure 8. Plot of formic acid concentration achieved after4 h vs. CO_2 pressure at several values of current density (range 7.8- 50 mA cm^{-2}). Comparison of the experimental *[HCOOH]* with the theoretical *[HCOOH]* at several value of current density: 7.8 (—); 20 (– – –); 30 (— — —); 50 (•••) mA cm^{-2}. Theoretical HCOOH concentration was evaluated under the assumptions described in the section 2.2.1 with the following fitting parameters: $k'(E)/k_4(E)$ = 0.18; $k_{an}'(E)/k_{HCOOH}(E)$ = 0.3 M; b = 1. Experimental data are from literature [40].

2.3.3. Effect of the time

In order to evaluate better the contribution of the anodic oxidation of HCOOH, the results of a long electrolysis previously reported by the authors [40] is compared with the previsions of the theoretical model in fig. 9.

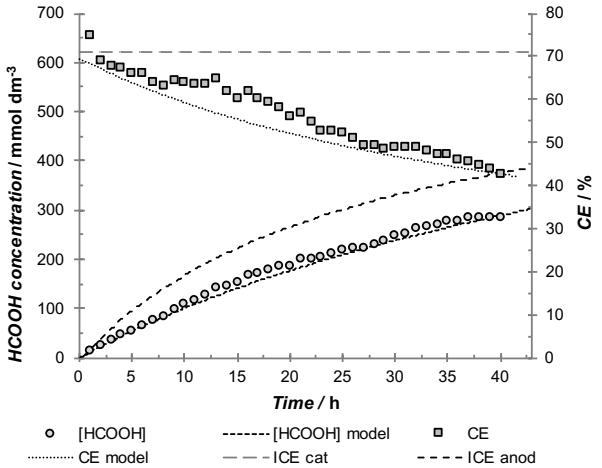

Figure 9. Comparison of the experimental generation of HCOOH and of the relative CE with the theoretical model. Experimental data are from literature [40].

The model well describes the evolution of the concentration of formic acid vs. time and the overall CE observed for long electrolyses for undivided cells [40]. In particular, CE decreases from an initial value close to 70% to a final one close to 42 % [40]. According to the proposed theoretical model, the trend of CE is due to the fact that the formation of HCOOH occurs with a constant ICE of about 70% while the anodic oxidation of HCOOH occurs with an increasing ICE (from 0 to about 44 %) due to the enhancement of the concentration of formic acid in the solution with the time passed.

2.3.4. Effect of the reactor and mixing rate

In order to evaluate the robustness of the proposed model, the theoretical predictions based on fitting parameters evaluated in paragraph 2.3.1 for a filter press cell with continuous recirculation of the pressurized solution with an area of tin cathode A of 9 cm^2 and a volume V of 0.9 L were compared with results achieved in a very different reactor after 6 h: a batch cell with a volume of 0.05 L, an area of the tin electrode of 4.5 cm^2 and no mixing (data reported in [39]). As shown in fig. 10a, in spite of the drastic change of reactor, ratio A/V and flow-dynamic regime, a quite good agreement between the theoretical model (here used in a fully predictive mode) and the experimental results is achieved. Please, consider that also in this case experimental data relative to regions 2 and 3 were selected.

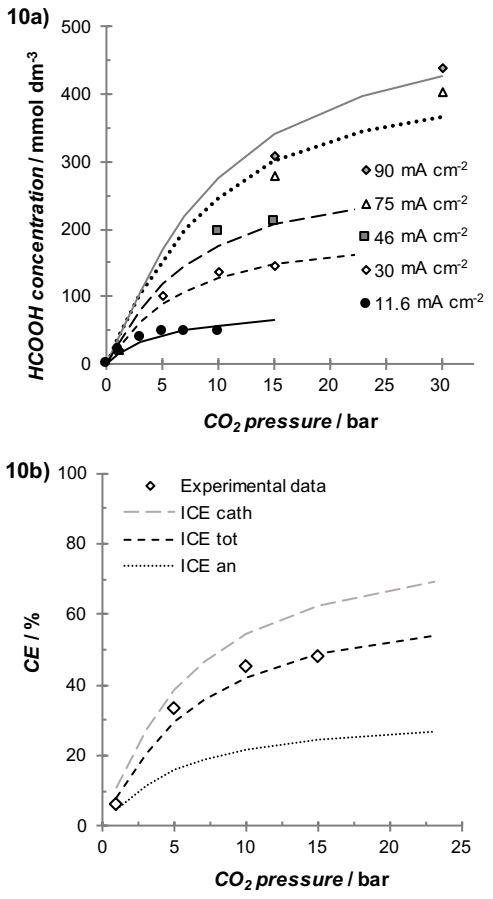

Figure 10 (10a) Plot of formic acid concentration vs. CO_2 pressure at several values of current density (range 11.6 - 90 mA cm^{-2}). Comparison of the experimental *[HCOOH]* achieved after 6 h with the theoretical *[HCOOH]* at several value of current density: 11.6 (—); 30 (– – –); 46 (— — —); 75 (•••); 90 (—); mA cm^{-2}. (10b) Plot of experimental CE and theoretical CE prediction vs CO_2 pressure at 30 mA cm^{-2}. Theoretical [HCOOH] and CE were evaluated under the assumptions described in the section 2.2.1 with the following fitting parameters: $k'(E)/k_4(E)$ = 0.18; $k_{an}'(E)/k_{HCOOH}(E)$ = 0.3 M; b = 1. Experimental data are from literature [39].

In particular, in this case very high HCOOH concentrations were achieved using both high pressures and *j*, because of the high ratio A/V. Fig. 10b reports a comparison between the experimental CE achieved after 6 h at 30 mA cm^{-2} and different pressures and the CE predicted by the model. A quite good agreement is observed also in this case; in particular, the theoretical CE increases with the pressure and it is significantly lower than the cathodic ICE, related to the formation of HCOOH, since a significant anodic ICE, relative to the anodic oxidation of HCOOH, occurs.

Conclusions

Electrochemical conversion of CO_2 at a tin cathode is considered a promising route for the production of formic acid. Here, a theoretical model was developed in order to describe the process and to evaluate the effect of operative parameters. In order to develop the model, a reaction mechanism and the relative r.d.s. have to be assumed. Hence, a large series of polarization and electrolyses was performed at various pressures in order to evaluate the kinetic of the process. According to the literature and experimental results, the reduction of pressurized CO_2 at a tin cathode can be described by a simple reaction mechanism, which involves the following key stages: (i) mass transfer of CO_2 to the cathode; (i) its adsorption described by a Langmuir equation; (iii) cathodic reduction of adsorbed CO_2 to adsorbed $CO_2^{\bullet-}$; (iv) cathodic reduction of adsorbed $CO_2^{\bullet-}$ to HCOOH. In particular, for not too low or too high current densities, the process is likely to be kinetically controlled by the mass transfer or the first reduction stage, depending on the value of the P_{CO_2}. Hence, a simple first-approximation model was developed based on these r.d.s. for the cathodic conversion of pressurized CO_2 to HCOOH and taking in account that HCOOH can be consumed by anodic oxidation in undivided cells. The theoretical model was in a good agreement with experimental results collected in this work and in previous ones and it well describes the effect of several operative parameters, including current density and pressure, time passed, kind of reactor and flow-dynamic.

Experimental Section

Electrochemical characterization

LSV and CV characterizations were performed by using: I) a conventional three-electrode cell with a Saturated Calomel Electrode reference and a Pt wire counter electrode; and II) an AISI316 stainless steel cell with a

cylindrical geometry, described in detail in a previous work [39]. The latter was used to carry out the pseudo-polarization curves at CO_2 pressure higher than the atmospheric one by changing the overall cell potential. The working electrode was a tin foil (0.1 cm^2); before each characterization, it was subjected to mechanically smoothing treatment, chemically pre-treated with 11 %vol HNO_3 (Romil Chemicals) water solution for 2 min and washed with an ultrasound bath in bi-distillate water for 5 min. The electrolyte solution was a 0.1M Na_2SO_4 (Janssen Chimica) aqueous solution (V = 0.05 L). The characterizations were performed at several values of mixing rate (0 - 600 rpm), of CO_2 pressure (1- 30 bar) and at different pH values, i.e. 2, 3 and 4; H_2SO_4 (Sigma Aldrich) was used to set the pH. Stirring of the solution was made with a magnetic stirrer. Prior to all characterization, the solution was purged for 25 minutes by either N_2 (99.999% purity; supplied by Air Liquide) or CO_2 (99.999% purity; supplied by Rivoira).

The partial current of CO_2 reduction j_{CO_2} was computed under the assumption that the current of the hydrogen evolution and of the CO_2 reduction can add up and the only competitive route to the CO_2 cathodic reaction is the hydrogen evolution. LSVs and CVs were acquired with a scan rate of 0.005 and 0.030 V s^{-1}, respectively, using an AutoLab PG-STAT12.

Electrolyses

Two different electrochemical set-up were used to carry out the reduction of CO_2. Set-up I was a batch undivided stainless steel cell, fitted out a tin foil cathode with a working area of 0.1 or 4.5 cm^2, and a DSA counter electrode, with magnetic stirring [39]. Set-up II was a pressurized undivided filter-press cell with parallel electrodes with a continuous recirculation system of the electrolytic solution, described in detail in our previous work [40]. The system was equipped with a centrifugal pump (MicroPump GHA-V21 with a maximum power pumping of 200 mL min^{-1}) and a stainless steel tank equipped with three connecting lines in the top (one for the CO_2 input, one for the products gas phase output and one connected with the bottom line for the circulation of the liquid phase) and a parallel line to the tank, equipped with a view-cell to check the liquid level in the system. The filter-press cell was provided with a tin sheet cathode ($A_{cathode}$= 9 cm^2, assay > 99%, Carlo Erba) and a Ti/IrO_2-Ta_2O_5 sheet anode (ElectroCell AB). The electrolytic solution was 0.1M Na_2SO_4 aqueous solution. The volume of the solution was 0.05 or 0.9 L, respectively, for the set-up I or II. To feed and pressurize the two systems, CO_2 99.999% (supplied by Rivoira) was employed. Electrolyses were carried out under amperostatic mode (Amel 2053 potentiostat/galvanostat) at room temperature.

The stagnant layer's thickness was evaluated through a well-know diffusion limiting current technique using a very stable redox couple (i.e., Fe^{2+}/Fe^{3+}). An electrolytic solution of $K_4Fe(CN)_6$ thrihydrate 99% (Carlo Erba reagents) and $K_3Fe(CN)_6$ 99% (Merk) at the same concentrations, i.e. 20, 40 and 80 mM, was used. To estimate the thickness value under adopted the condition, the diffusion coefficients in aqueous solution were assumed of 6.631*10^{-6}, 1.85*10^{-5} and 1*10^{-5} cm^2 s^{-1}, respectively, for the redox couple [47], CO_2 [48] and formic acid [40].

The performances of the process were discussed in term of the current efficiency (CE) and the rate of formic acid generation. The CE and the instantaneous current efficiency (ICE) were defined, as follows:

$$\boldsymbol{CE = 2\,F\,[HCOOH]_t\,V/I\,t};$$

$$\boldsymbol{ICE = 2\,F\,([HCOOH]_{t+\Delta t} - [HCOOH]_{\Delta t})\,V/I\,\Delta t}$$

where F is the faradaic constant (96487 C mol^{-1}), $[HCOOH]_t$ the concentration of formic acid at the time t, V the solution volume and I the current.

The formic acid production rate was expressed as the formic acid produced per unit of the working area and unit of time (mmol h^{-1} cm^{-2}). To evaluate the formic acid concentration, Agilent HP 1100 HPLC fitted out with Rezex ROA-Organic Acid H+ (8%) column at 55 °C and coupled with a UV detector (210 nm) was used; 0.005N H_2SO_4 water solution at pH 2.5 was eluted at 0.6 mL min^{-1} as mobile phase. The gas products were analized by gas cromathography using a Agilent 7890B GC fitted out with a Supelco Carboxen® 60/80 column and a thermal conductivity detector (TCD), working at 230°C. Helium (99.999%, Air Liquide) at 1 bar was used as carrier gas. The temperature of the column was programmed, that is: an isotherm at 35°C for 5 min followed by a 20°C/min ramp up to 225°C and by an isothermal step for 40 min.

Abbreviations

$[CO_2]^0$	Surface electrode CO_2 concentration
$[CO_2]^b$	Bulk CO_2 concentration
$[HCOOH]^0$	Surface electrode HCOOH concentration
$[HCOOH]^b$	Bulk HCOOH concentration
CE	Current Efficiency
F	Faraday constant
ICE	Istantaneous Current Efficiency
j	Current density
j_{HCOOH}	HCOOH oxidation current density
j_{CO_2}	CO_2 partial current density
j_{lim}	Limiting current density
$j_{wat,an}$	Water oxidation current density
$k'(E)$	Product of the heterogeneous rate constant for the water reduction and water concentration
$k_4(E)$	Heterogeneous rate constant for the CO_2 adsorded reduction
$k_{an}'(E)$	Product of the heterogeneous rate constant for the water oxidation and water concentration
$k_{HCOOH}(E)$	Heterogeneous rate constant for the HCOOH oxidation
k_m	CO_2 mass transfer coefficient
$k_{m,HCOOH}$	HCOOH mass transfer coefficient
N	Mixing rate
P_{CO_2}	CO_2 pressure
θ	Surface coverage degree
r_{CO_2}	Rate of CO_2 cathodic conversion to HCOOH
r_{HCOOH}	HCOOH oxidation rate
t	Time
V	Volume of solution

Acknowledgements

University of Palermo is acknowledged for its financial support.

Keywords: CO_2 • Pressure • Reduction • Theoretical Model • Tin

[1] H. R. M. Jhong, S. Ma, P.J. Kenis, *Curr. Opin. Chem. Eng.* **2013**, 2, 191-199.
[2] D. T. Whipple, P. J. A. Kenis, *J. Phys. Chem. Lett*. **2010**, 1, 3451-3458.
[3] J. S. Yoo, R. Christensen, T. Vegge, J. K. Norskov, F. Studt, *ChemSusChem.* **2016**, 9, 358-363.
[4] M. Jitaru, D. A. Lowy, M. Toma, B. C. Toma, L. Oniciu, *J. Appl. Electrochem.* **1997**, 27, 875–889.
[5] E. J. Dufek, T. E. Lister, M. E. McIlwain, *J. Appl. Electrochem*. **2011**, 41, 623-631.
[6] Y. Chen, C. W. Li, M. W. Kanan, *J. Am. Chem. Soc.* **2012**, 134, 19969-19972.
[7] J. Albo, M. Alvarez-Guerra, P. Castaño, A. Irabien, *Green Chem*. **2015**, 17, 2304-2324.
[8] P. G. Russell, N. Kovac, S. Scrinivasan, M. Steinberg, *J. Electrochem. Soc.* **1977**, 124, 1329-1338.
[9] F. Koleli, D. Balun, *Appl. Catal., A* **2004**, 274, 237-242.
[10] W. Lv, R. Zhang, P. Gao, L. Lei, *J. Power Sources.* **2014**, 253, 276-281.
[11] R. Zhang, W. Lv, L. Lei, *Appl. Surf. Sci.* **2015**, 356, 24-29.
[12] Y. Chen, M. W. Kanan, *J. Am. Chem.Soc.* **2012**, 134, 1986-1989.
[13] P. Bumroongsakulsawat, G.H. Kelsall, *Electrochim. Acta.* **2015**, 159, 242-251.
[14] Y. Hori, K. Kikuchi, S. Suzuki, *Chem. Lett.* **1985**, 11, 1695-1698.
[15] M. Azuma, K. Hashimoto, M. Hiramoto, M. Watanabe, T. Sakata, *J. Electrochem. Soc.* **1990**, 137, 1772-1778.
[16] S. Ikeda, T. Takagi, K. Ito, *Bull. Chem. Soc. Jpn*. **1987**, 60, 2517-2522.
[17] W. Lv, R. Zhang, P. Gao, C. Gong, *J. Solid State Electrochem.* **2013**,17, 2789-2794.
[18] A. Gennaro, A. A. Isse, M.-G. Severin, E. Vianello, I. Bhugun, J.-M. Savéant, *J. Chem. Soc., Faraday Trans.* **1996**, 92, 3963-3968.
[19] O. Scialdone, A. Galia, A. A. Isse, A. Gennaro, M. A. Sabatino, R. Leone, G. Filardo, *J. Electroanal. Chem.* **2007**, 609, 8-16.
[20] O. Scialdone, A. Galia, G. Errante, A. A. Isse, A. Gennaro, G. Filardo, *Electrochim. Acta.* **2008**, 53, 2514-2528.
[21] O. Scialdone, G. Filardo, A. Galia, D. Mantione, G. Silvestri, *Acta Chem. Scand*. **1999**, 53, 800-806.
[22] O. Scialdone, A. Galia, C. La Rocca, G. Filardo, *Electrochim. Acta.* **2005**, 50, 3231-3242.
[23] D. Du, R. Lan, J. Humphreys, S. Tao, *J. Appl. Electrochem.* **2017**, 46, 661-678.
[24] S. Sabatino, A. Galia, G. Saracco, O. Scialdone, *ChemElectroChem.* **2017**, 4, 150-159.
[25] E. Irtem, T. Andreu, A. Parra, M. D. Hernàndez-Alonso, S. García-Rodríguez, J. M. Riesco-García, G. Penelas-Pérez, J.R. Morante, J. *Mater. Chem. A* **2016**, 4, 13582-13588.
[26] D. Kopljar, A. Inan, P. Vindayer, N. Wagner, E. Klemm, *J. Appl. Electrochem*. **2014**, 44, 1107-1116.
[27] M. Alvarez-Guerra, A. Del Castillo, A. Irabien, *Chem. Eng. Res. Des.* **2014**, 92, 692-701.
[28] A.S. Agarwal, Y. Zhai, D. Hill, N. Sridhar, *ChemSusChem.* **2011**, 4, 1301-1310.
[29] K. Ohta, A. Hasimoto, T. Mizuno, Energy Convers. Manage. **1995**, 36, 625-628.
[30] Anawati, G.S. Frankel, A. Agarwal, N. Sridhar, *Electrochim. Acta*. **2014**, 133, 188-196.
[31] J. Wu, S. G. Sun, X.D. Zhou, Nano Energy. **2016**, 27, 225-229.
[32] Y. Wang, J. Zhou, W. Lv, H. Fang, W. Wang, *Appl. Surf. Sci.* **2016**, 362, 394-398.
[33] A. Q. Fenwick, O. R. Luca, *J. Photochem. Photobiol. B Biol.* **2014**, 152, 43-46.
[34] Q. Wang, H. Dong, H. Yu, *J. Power Sources.* **2014**, 271, 278-284.
[35] A. Del Castillo, M. Alvarez-Guerra, J. Solla-Gullon, A. Sàez, V. Montiel, A. Irabien, *J. CO_2 Util.* **2017**, 18, 222-228.
[36] K. Hara, A. Kudo, T. Sakata. *J. Electroanal. Chem.* **1995**, 391,141-147.
[37] M. Todoroki, K. Hara, A. Kudo, T. Sakata. *J. Electroanal. Chem.* **1995**, 394, 199-203.
[38] Yu. B. Vassiliev, V.S. Bagotzky, N.V. Osetrova, O.A. Khazova, N. A. Mayorova. *J. Electroanal Chem.* **1985**, 189, 271-294.
[39] O. Scialdone, A. Galia, G. L. Nero, F. Proietto, S. Sabatino, B. Schiavo, *Electrochim. Acta.* **2015**, 199, 332-341.
[40] F. Proietto, B. Schiavo, A. Galia, O. Scialdone, *Electrochim. Acta.* **2018**, 277, 30-40.
[41] P. Bumroongsakulsawat, G. H. Kelsall. *Electrochim. Acta*. **2014**, 14, 216-225
[42] M. F. Baruch, J. E. Pander III, J. L. White, A. B. Bocarsly. *ACS Catal*. **2015**, 5, 3148-3156
[43] W. Paik, T. N. Andersen, H. Eyring, *Electrochim. Acta*. **1969**, 14, 1217-1232.
[44] Y. Zhang, L. Chen, F. Li, C. D. Easton, J. Li, A. M. Bond, J Zhang. *ACS Catal.* **2017**, 7, 4846-4853.
[45] R. P. S. Chaplin, A. A. Wragg, *J. Appl. Electrochem*. **2003**, 33, 1107-1123
[46] R. Kortlever, J. Shen, K. J. P. Schouten, F. Calle-Vallejo, M. T. M. Koper, *J. Phys. Chem. Lett.* **2015**, 6, 4073-4082.
[47] A. A. Wragg, A. A. Leontaritis, *Chem. Eng. J.* **1997**, 66, 1-10.
[48] A. Tamimi, E.B. Rinker, O.C. Sandall, *J. Chem. Eng. Data.* **1994**, 39, 330-332.
[49] O. Azizi, M. Jafarian, F. Gobal, H. Heli, M.G. Mahjani, *Int. J. Hydrogen Energy*. **2007**, 32, 1755-1761.
[50] O. Scialdone, *Electrochim. Acta*. **2009**, 54, 6140-6147.
[51] O. Scialdone, A.Galia, S. Randazzo, *Chem. Eng. J.* **2012**, 183, 124-134.

Entry for the Table of Contents (Please choose one layout)

Layout 1:

ARTICLE

A simple theoretical model was developed to describe the electrochemical reduction of pressurized carbon dioxide at tin cathode in an undivided cell. The theoretical model was in a good agreement with experimental results and well described the effect of several operative parameters, including current density, pressure and kind of reactor.

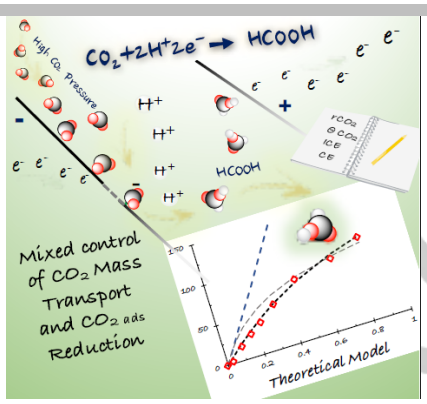

*Federica Proietto, Alessandro Galia and Onofrio Scialdone**

Page No. – Page No.

Electrochemical conversion of CO_2 to HCOOH at tin cathode: development of a theoretical model and comparison with experimental results

Layout 2:

ARTICLE

((Insert TOC Graphic here))

Page No. – Page No.

Title

Text for Table of Contents